PHYSICAL REVIEW E VOLUME 57, NUMBER 4 APRIL 1998

Reactive wetting- and dewetting-induced diffusion-limited aggregation

D. W. Zheng, Weijia Wen, and K. N. Tu
Department of Materials Science and Engineering, UCLA, Los Angeles, California 90095-1595
(Received 21 October 1997; revised manuscript received 17 December 1997)

Diffusion-limited-aggregation-like fractals, formed by the wetting of an eutectic SnPb alloy ball on an Au/Cu/Cr multilayered thin film and the dewetting of SnPb from the Cr surface after the Au/Cu thin film underneath the wetting cap was consumed, have been observed experimentally. The wetting-formed fractal is inside the precursor of the SnPb wetting cap, while the dewetting-formed fractal sits around the center of the SnPb cap. A unique characteristic of the former is that its growth direction is opposite to the wetting direction of the SnPb. More interestingly, the latter seems to be a reverse process of the regular fractal formation, and it ends up with a diffusion-limited-aggregation-like pattern. The dimensions of the two fractal patterns are measured to be 1.83 ± 0.07 and 1.79 ± 0.06. Their formation mechanisms are discussed in terms of diffusion-limited aggregation and its reverse process, respectively. [S1063-651X(98)50104-3]

PACS number(s): 68.45.−v, 61.43.Hv, 61.16.Bg

A large variety of natural phenomena encountered in physics, chemistry, and biology are attributed to diffusion processes. Fractals induced by diffusion phenomena have attracted much attention in the past decade [1–5]. There exist several different kinds of diffusion-induced fractals. Fractal growth based on the mechanism of diffusion-limited aggregation (DLA), which involves Brownian motion of particles, was first introduced by Witten and Sander [6]. This mechanism has been tested experimentally in various fields, such as crystal growth, electrochemical deposition, viscous fingering, and dielectric breakdown, which are all governed by the same growth rule [7–10]. Another kind of diffusion-limited-aggregation fractal reported recently was named as *field-induced* DLA, where the fractal patterns are caused by the dipole interaction of particles under the magnetic or electric field [11,12]. Furthermore, fractal formation during the solidification process, which involves precipitate diffusion and irreversible aggregation, has drawn much more attention regarding the transition between a stable growth of traditional dendritic or cellular pattern and fractal pattern [13,14].

In this paper we report experimental phenomena of fractal pattern formation by the reactive wetting and dewetting of an eutectic SnPb binary alloy on *smooth* Au/Cu/Cr multilayered thin films. We demonstrate that in wetting, the wetting front of the eutectic SnPb alloy has an unusual fractal character upon solidification; the fractal grows against the wetting direction, from the wetting front to the center of the cap. However, in dewetting, which occurs when the molten SnPb alloy consumes all the Au/Cu thin film and reaches the unwettable Cr surface, fractal patterns are formed by the Sn-Pb leftovers on Cr.

P-type (100) Si wafers with 3000 Å of thermally grown SiO_2 were used as the substrates. Films of Cr, Cu, and Au were sputtered sequentially onto the SiO_2 under a base pressure of less than 2×10^{-7} torr, and formed a layered structure of Au(500 Å)/Cu(1 μm)/Cr(800 Å), where Au was the top layer. During reflow testing, a SnPb ball of a certain weight, together with the substrate, was put into a container with circular openings at the bottom. The container was then immersed in RMA 197 soldering flux (Kester Co.) inside a beaker that sat on top of a hot plate which was kept constant at 250 °C. The flux temperature difference between the bottom and top of the beaker caused natural circulation of flux, which brought fresh flux to the sample surface. Samples were taken out of the beaker after the scheduled time and cooled down to room temperature before being cleaned in ethyl alcohol.

Figure 1(a) is a schematic cross-sectional diagram that shows an early stage of wetting of an eutectic SnPb cap on the Au/Cu/Cr layered thin film. The cap has a diameter of approximately 2.8 mm. Experimentally, it was observed that the wetting angle (about 9°) did not change with reflow time while a very thin precursor band (less than 0.1 μm thick here), called ''sideband,'' kept growing larger from the edge of the SnPb cap. A scanning electron microscope (SEM) with energy-dispersive x-ray analysis (EDX) was used to detect the chemical composition of the sideband after the sample was cooled down from the reaction temperature. It was determined that at the front edge of the sideband there was a band of Pb islands. In between the front edge of the sideband and SnPb cap there existed a distribution of Sn, Pb, Cu, and a very small amount of Au. Figure 1(b) is a SEM backscattering image of the sideband and solder cap edge, where the dendritic pattern can be observed near the SnPb cap edge after 1 min at 250 °C. Its composition was determined by EDX to be a Pb-rich PbSn alloy. Figure 1(c) shows the wetting edge of another sample after 20 min at 250 °C. The treelike fractal can be seen clearly and is also a Pb-rich PbSn alloy. At higher magnification we can determine that the Pb fractal formed at the surface and the matrix surrounding it has the characteristic complex lamellar phase of SnPb eutectic. We notice not only that the shapes of the Pb(Sn) precipitates in the two cases are different, but also that their starting-edge locations are different. The dendritic pattern in Fig. 1(b) is quite common for precipitates during directional solidification. Due to the short wetting time, we find only Pb islands at the sideband tip, which can be identified by the narrow white coastline in Fig. 1(b). It is easily understood that Sn was depleted by the reaction with Au/Cu underneath the SnPb cap, and the excess Pb would precipitate out during solidification. However, the fractal pattern of the Pb(Sn) precipitate in Fig. 1(c) deserves more explanation.

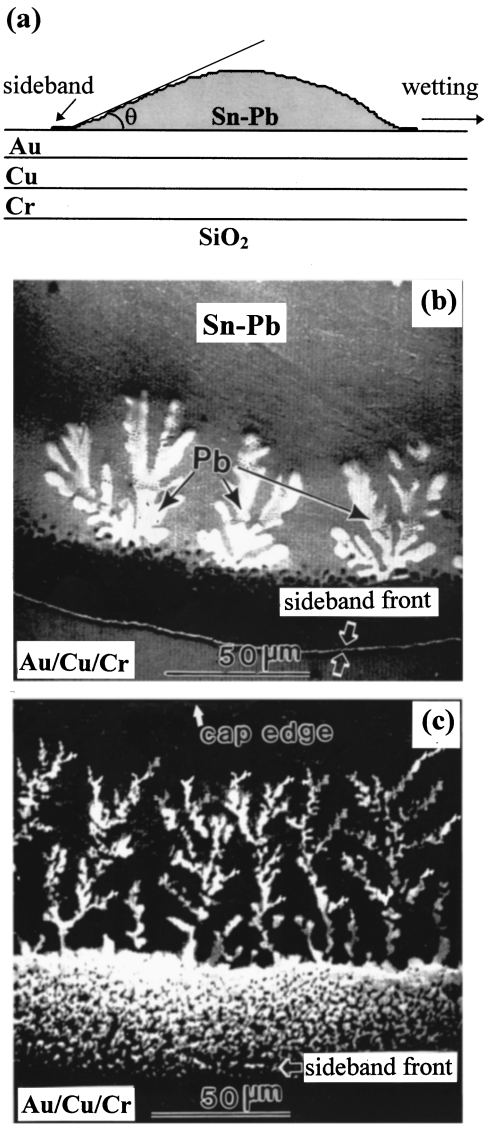

FIG. 1. (a) Schematic diagram showing the side view of the SnPb alloy cap wetting on Au/Cu/Cr layered thin film (not to scale); (b) fractal-like pattern of a Pb-rich alloy formed after 1 min at 250 °C; (c) treelike fractal of a Pb-rich alloy formed after 20 min at 250 °C.

Experimentally, it has been observed that the sideband is a very thin layer and that its formation can be explained only by the diffusion of a very small amount of SnPb out of the SnPb alloy cap and the reactions with the Au/Cu both laterally at the sideband tip and in depth everywhere in the sideband. The measured sideband growth rate corresponds to a diffusivity of 15×10^{-8} cm^2/sec at 250 °C, which may suggest a surface diffusion mechanism. Since the reaction temperature is above the eutectic point of 183 °C and below the melting point of Pb (327.5 °C), SnPb must form a couple and come out of the SnPb cap together. An *in situ* Auger-electron-spectroscopy (AES) study of the sideband that formed during eutectic SnPb wetting on bulk Cu [15], which is a similar system, showed a decreasing surface concentration profile of Sn and Pb from the SnPb cap edge to sideband edge. It seems that the Pb-rich precipitates in Fig. 1(c) have a concentration gradient that is opposite to the diffusion direction of either Sn or Pb. This can be understood if you realize that the local Pb/Sn ratio could decrease from the sideband tip to the SnPb cap edge, due to the fact that the sideband tip has Sn depletion due to the fast reaction with Au/Cu. However, closer to the solder cap edge, the reaction was in the vertical direction and had to go through the thicker diffusion barrier of the already-formed Cu-Sn compound [16].

Another key question has to do with when the fractal is formed. We hypothesize that it is most likely formed during solidification, not during the high-temperature reaction. The SnPb phase diagram [17] indicates that at 250 °C the system can tolerate a Pb enrichment up to 67 wt% from its 37 wt% eutectic composition without Pb(Sn) precipitation. During solidification, due to the local Pb/Sn ratio distribution at the sideband tip, where this ratio is the highest, Pb(Sn) precipitated out first, and formed a band of islands. Pb precipitation occurs later and there is less of an excess of Pb as the ratio distribution moves closer to the solder cap. Since Pb has to diffuse a long distance to aggregate, some fluctuation in the system could trigger the fractal pattern formation. But this fractal could only extend a certain distance into the sideband and it stopped when the excess amount of Pb was too little. This entire process involves the diffusion of Pb and the irreversible aggregation of Pb, which is a typical DLA system. There are some experimental reports [13] and modeling work on fractal pattern formation during solidification [14]. The uniqueness of our system is that the solidification, which is similar to that of constitutional supercooling, is governed mainly by the chemical-reaction-induced depletion of Sn, not just the temperature gradient as in a directional solidification system. In addition, since the solder cap has a much larger heat capacity than the sideband, there can be a lateral temperature gradient that enhances the directional solidification. It is emphasized that the dendritic and treelike fractal Pb precipitates were observed in the same system and their formation mechanism was hypothesized to be the same, which agrees with the point of view [6] that the diffusion-limited-aggregation fractal is a discrete version of dendritic growth, where the fluctuation in the diffusion field is high.

Figure 2(a) depicts the case where 0.5 mg of eutectic SnPb dewets from the center of the cap after all of the Au/Cu underneath the cap has been consumed at 250 °C, and the Cr surface is exposed. Figures 2(b)–2(d) show a series of SEM backscattering images indicating the evolution of the fractal formation during dewetting at different time steps. As reported by a previous study [16], during the reaction, Au dissolved into the molten SnPb (note that the amount of Au is very small) and SnCu compound (Cu_6Sn_5) formed with scallop-type grains and, at the same time, ripening occurred among them. Owing to the finite amount of Cu, the Cu_6Sn_5 eventually transformed into spheroids and spalled away from the interface, so that the molten SnPb contacted the Cr, which is an unwettable surface, and caused dewetting. Figure 2(b) is the case after 10 min and Fig. 2(c) is the case after 20 min where we can see that dewetting has begun at numerous spots. We note that the dark area is Cr on SiO_2 film, where SnPb has moved away and exposed the Cr to flux. The migration of the SnPb mass from the center to the edge is quite obvious, and we believe that the SnAu/Cu reaction at the edge reaction front could lower the system's Gibbs free en-

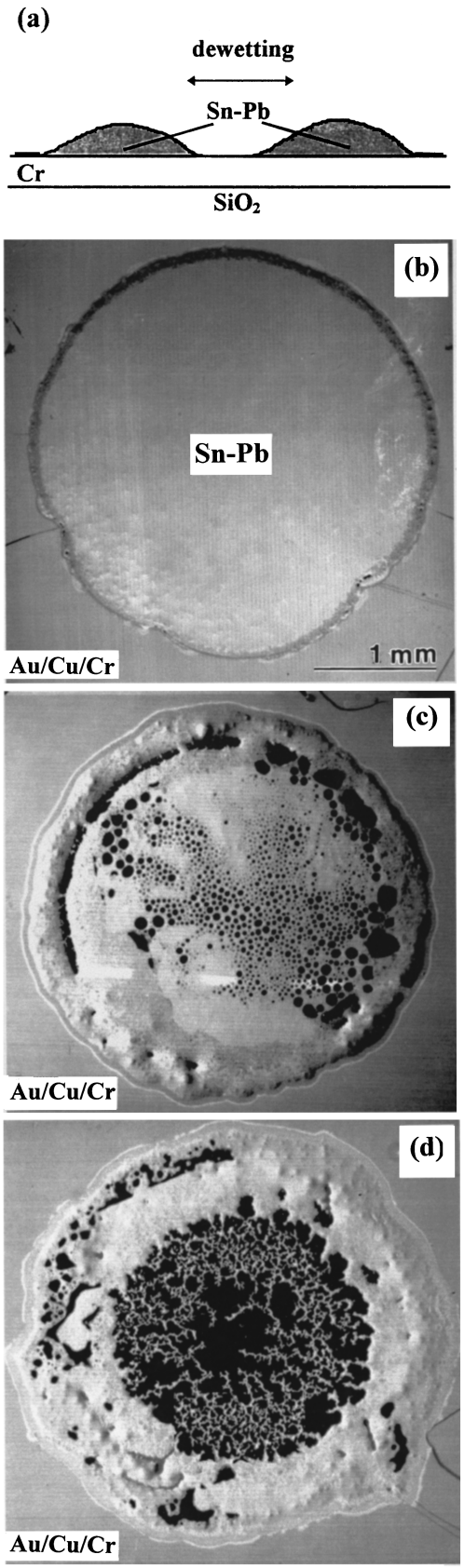

FIG. 2. (a) Schematic diagram showing the side view of the SnPb alloy dewetting from the Cr layer after the Au/Cr thin film underneath the SnPb cap is consumed (not to scale); (b)–(d) SEM backscattering image of SnPb cap wetting on Au/Cu/Cr thin film at 250 °C after 10, 20, and 30 min, respectively.

ergy and work as the driving force for this mass migration. Eventually, the pattern of the SnPb left at the center of the cap forms fractals, which is the situation after 30 min of reaction as revealed in Fig. 2(d). A cross-section study of these fractals shows typically one or two Cu_6Sn_5 particles wrapped by nearly eutectic SnPb. This is because the thickness of the SnPb that is left is so small that there is insufficient buoyancy force, and also, in ripening distribution, the larger Cu_6Sn_5 particles survive. Where the CuSn compounds remain, they provide adhesion between the SnPb on top and the Cr beneath.

From Fig. 2(c) and Fig. 2(d), it can be seen that two different processes occur. First, locally Cu_6Sn_5 continues to spall away from some sites at the center part and allows the SnPb on top to move away. As the molten SnPb moves, the CuSn compound that it wraps around will be carried away. We hypothesize that the above process can be equivalently viewed as the ripening of the dark Cr exposed area, which is rather similar to grain growth if we regard each of the exposed areas as a grain. Globally, SnPb will diffuse to the edge of the solder cap and the cap grows bigger. The SnPb flow has to be accomplished through the interconnected fractal branches. This fractal formation is quite unique. It seems to be a reverse of the generic fractal-formation-like DLA process. For regular DLA, a random-walk particle gets stuck when it touches the growing aggregate branches. It starts with one seed and ends up with a fractal-covered surface. In our process, initially all the SnPb eutectic alloy can sit on top of the CuSn compound. Due to the reaction and ripening fluctuation and nonplanar nature of the Cu_6Sn_5 formed, we end up with only some fractal shape of SnPb. Even though diffusion might be the limiting process in both systems, there seems to be more restriction to the diffusion process in our system as compared to the regular DLA, which has unlimited diffusion paths. More detailed dynamics study needs to be carried out. Actually this fractal is a metastable state. If we heat the sample substantially at 250 °C for 70 min, all fractals of SnPb at the center are gone and a dark circular area of Cr is left at the center. The mechanism that takes SnPb out of the center area is the reduction of surface energy and chemi-

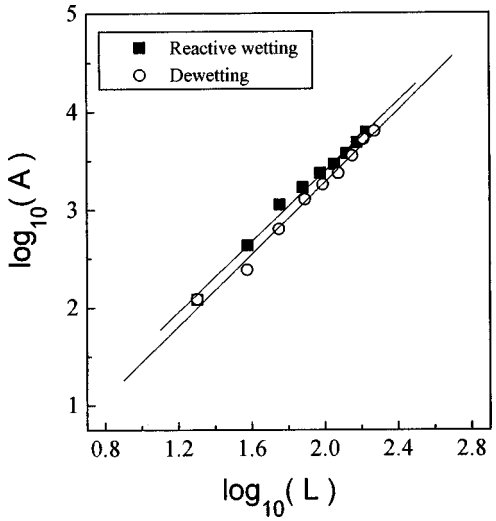

FIG. 3. Fractal area vs sampling box side length (in pixels), where the square symbol represents the case of wetting and the circular symbol represents the case of dewetting.

cal reaction at the peripheral area of the solder cap. Also, we note that this mode of dewetting is unexpected. This is because if we only consider the reduction in surface energy, the half-donut shape of the SnPb alloy will not be the minimum-energy configuration, which should be a cap of larger wetting angle.

The dimensions of the two fractal patterns formed in Figs. 1(c) and 2(d) are obtained using the equation $A = L^{D_f}$, where A is the area of the Pb (SnPb) fractal, L is the side length in number of pixels of the sampling square box and D_f is the dimension of the fractal. The fractal image was obtained in 256 grayscale digital format and converted to binary grayscale format after appropriate grayscale criteria were chosen such that all of the fractal area turned out to be white (255 in grayscale) and the background was dark (0 in grayscale). By varying the length L while calculating the number of pixels covered by the fractal, we obtained the D_f from the slope of $\log_{10}(A)$ versus the $\log_{10}(L)$ curve shown in Fig. 3. The numerical result is that the dimension of fractal formed during reactive wetting is 1.79 ± 0.06 for Fig. 1(c), while the dimension of fractal induced by dewetting is 1.83 ± 0.07 for Fig. 2(d). Although the geometric outlooks of the two fractals are somehow not alike, their fractal dimensions are pretty close.

In conclusion, we have demonstrated experimentally that the fractal pattern formation within the sideband during the reactive wetting of eutectic SnPb on Au/Cu/Cr and the dewetting of SnPb from the Cr surface after the Au/Cu thin film are consumed. The former is based on an equivalent constitutional supercooling caused by the composition gradient of Pb/Sn as a result of chemical reaction within the sideband. The latter is characterized by a reverse process of general fractal formation where the driving force to take the particles out of the area of interest is again the chemical reaction at the cap edge.

[1] T. Vicsek, *Fractal Growth Phenomena* (World Scientific, Singapore, 1989).

[2] A. Kuhn, F. Argoul, J. F. Muzy, and A. Arneodo, Phys. Rev. Lett. **73**, 2998 (1994).

[3] R. Jullien, J. Phys. A **19**, 2129 (1986).

[4] M. B. Mineev-Weinstein and R. Mainieri, Phys. Rev. Lett. **72**, 880 (1993).

[5] T. C. Halsey, Phys. Rev. Lett. **72**, 1228 (1993); D. S. Graff and L. M. Sander, Phys. Rev. E **47**, 2273 (1993); H. Kaufman, A. Vespingnani, B. B. Mandelbrot, and L. Woog, *ibid.* **52**, 5602 (1995).

[6] T. A. Witten and L. M. Sandar, Phys. Rev. Lett. **47**, 1400 (1981).

[7] Y. Saito, G. Goldbeck-Wood, and H. Muller-Krumbhaar, Phys. Rev. Lett. **58**, 1541 (1987).

[8] M. Matsushita, M. Sano, Y. Hayakawa, H. Honjo, and Y. Sawada, Phys. Rev. Lett. **53**, 286 (1984); D. G. Grier, E. Ben-Jacob, R. Clare, and L. M. Sander, *ibid.* **56**, 1264 (1986).

[9] J. E. Fernandez and J. M. Albarran, Phys. Rev. Lett. **64**, 2133 (1990).

[10] L. Niemeyer, L. Pietronero, and H. J. Wiesmann, Phys. Rev. Lett. **52**, 1033 (1984); **57**, 650 (1986).

[11] N. Vandewalle and M. Ausloos, Phys. Rev. E **51**, 597 (1995).

[12] W. Wen and K. Lu, Phys. Rev. E **55**, R2100 (1997); Phys. Fluids **9**, 1826 (1997).

[13] O. G. Mouritsen, Int. J. Mod. Phys. B **4**, 1925 (1990).

[14] Y. Saioto, T. Sakiyama, and M. Uwaha, J. Cryst. Growth **128**, 82 (1993).

[15] G. C. Smith and C. Lea, Surf. Interface Anal. **9**, 145 (1986).

[16] A. A. Liu, H. K. Kim, K. N. Tu, and P. A. Totta, J. Appl. Phys. **80**, 2774 (1996).

[17] *Binary Alloy Phase Diagrams*, edited by T. B. Massalski, H. Okamoto, P. R. Subramanian, and Linda Kacprzak (ASM International, Materials Park, Ohio, 1990).